Journal of Computations & Modelling, vol.2, no.4, 2012, 25-50
ISSN: 1792-7625 (print), 1792-8850 (online)
Scienpress Ltd, 2012

Soret and Dufour Numbers Effect on Heat and Mass Transfer in Stagnation Point Flow Towards a Stretching Surface in the Presence of Buoyancy Force and Variable Thermal Conductivity

M.A.A. Bazid[1], Z.M. Gharseldien[1,2], M.A. Seddeek[3] and M. Alharbi[4]

Abstract

A numerical study of heat and mass transfer in two-dimensional stagnation-point flow of an incompressible viscous fluid over a stretching vertical sheet in the present of thermal-diffusion (Soret) and diffusion-thermo (Dufour) numbers is investigated. The analysis accounts for both assisting and opposing flows and temperature dependent thermal conductivity. The set of governing equations and the boundary condition are reduced to ordinary differential equations with appropriate boundary conditions. Furthermore, the similarity equations are solved

[1] Department of Mathematics, Faculty of Science, Wadi Adawasir, Salman Bin Abdulaziz University, Saudi Arabia
[2] Department of Mathematics, Faculty of Science, Cairo, Al-Azhar University, Egypt
[3] Department of Mathematics, Deanship of Educational Services, Qassim University, P.O. Box 6595, Burieda 51452, Saudi Arabia
[4] Department of Mathematics, Faculty of Science, Umm AL-Qura University, Makkah, Saudi Arabia

Article Info: *Received* : September 5, 2012. *Revised* : October 23, 2012
Published online : December 30, 2012

numerically by using fourth order Runge-Kutta integration scheme with Newton Raphson shooting method. The accuracy of the numerical method is tested by performing various comparisons with previously published work and the results are found to be in excellent agreement. Numerical results for velocity, temperature and concentration distributions as well as skin friction coefficient, local Nusselt number and local Sherwood numbers are discussed for various values of physical parameters.

Mathematics Subject Classification: 76R10
Keywords: Heat and mass transfer, Boundary layer, Stagnation-point flow, Soret and Dufour Effects, Stretching sheet

1 Introduction

The heat, mass, and momentum transfer in the laminar boundary layer flow on stretching sheets are important from a theoretical as well as practical point of view because of their wider applications to polymer technology and metallurgy. During many mechanical forming processes, such as extrusion, melt-spinning, cooling of a large metallic plate in a bath, manufacture of plastic and rubber sheets, glass blowing, continuous casting, and spinning of fibers, the extruded material issues through a die. Sakiadis [1] initiated the study of the boundary layer flow over a flat surface moving with a constant velocity and formulated a boundary layer equation for the two dimensional and axisymmetric cases. Crane [2] studied the steady two dimensional flow caused by the stretching of an elastic flat surface which moves on its own plane with a velocity varying linearly with distance from a fixed point. The problem of flow and heat transfer over a stretching surface has been investigated and discussed by many researchers [3–10]. Stagnation flow, which describes the fluid motion near the stagnation region,

exists on all solid bodies moving in a fluid. There has been considerable interest in investigating plane and axisymmetric flow near a stagnation point on a surface. Hiemenz [1] was the first to discover that the stagnation point flow can be analyzed exactly by the Navier-Stokes equations, and he reported two-dimensional plane flow velocity distribution. Chiam [2] investigated two dimensional normal and oblique stagnation-point flows of an incompressible viscous fluid towards a stretching surface. Furthermore, the behavior of stagnation-point flow over stretching sheet under different physical aspects was discussed by Mahapatra and Gupta [8], Ishak et al. [9]-[10], Layek et al. [11] and Nadeem et al. [12], Rashidi and Erfani [13]. Recently, Afify and Elgazery [14] studied the effects of chemical reaction and suction/injection on MHD stagnation-point flow of heat and mass transfer towards a heated porous stretching sheet by using a scaling group of transformations. In all these studies Soret and Dufour effects were assumed to be negligible. When heat and mass transfer occur simultaneously in a moving fluid, the relations between the fluxes and the driving potentials may be of a more intricate nature. An energy flux can be generated not only by temperature gradients, but by composition gradients also. The energy flux caused by a composition gradient is termed the Dufour or diffusion-thermo effect. On the other hand, mass fluxes can also be created by temperature gradients and this embodies the Soret or thermal-diffusion effect. Such effects are significant when density differences exist in the flow regime. For example, when species are introduced at a surface in a fluid domain, with a different (lower) density than the surrounding fluid, both Soret (thermo-diffusion) and Dufour (diffuso-thermal) effects can become influential. Soret and Dufour effects are important for intermediate molecular weight gases in coupled heat and mass transfer in fluid binary systems, often encountered in chemical process engineering. The influence of species inter diffusion and also the Soret and Dufour effects on the natural convective heat and mass transfer in an enclosure due to mutual action of temperature and concentration gradients was investigated [20]. Dursunkaya and Worek [21] have

studied Soret/Dufour effects on both unsteady and steady natural convection from vertical surfaces. Chamkha and Ben-Nakhi [22] who analyzed the MHD mixed convection flow under the radiation interaction along a vertical permeable surface immersed in a porous medium in the presence of Soret and Dufour's effects. Seddeek [23] studied thermo-diffusion and diffusion-thermo effects on mixed convection flow over an accelerating surface with a heat source with suction/ blowing for the case of variable viscosity. Afify [24] studied the effects of thermal-diffusion and diffusion thermo with suction/injection on MHD free convective heat and mass transfer over a stretching sheet considering. Postelnicu [25] studied the simultaneous heat and mass transfer by natural convection in a two dimensional stagnation-point flow of a fluid saturated porous medium, using the Darcy–Boussinesq model, including suction/blowing, Soret and Dufour effects. Recently, Magyari and Postelnicu [26] studied the double-diffusive natural convection past a vertical plate embedded in a fluid-saturated porous medium with Soret–Dufour cross-diffusion effects. The objective of the present work is to investigate the heat and mass transfer in two-dimensional stagnation-point flow in the present of the effects of variable thermal conductivity with Soret and Dufour Numbers over a stretching vertical sheet. Both both assisting and opposing flows are considered in the study. The governing equations, describing the problem, are transformed into ordinary differential equations by using similarity transformations. These equations are more conveniently solved numerically by using fourth order Runge-Kutta integration scheme with Newton Raphson shooting method. The obtained results are shown graphically and the physical aspects of the problem are discussed.

2 Mathematical formulation

Consider the steady, two-dimensional laminar free convective flow of a

viscous and incompressible fluid near the stagnation point over continuously moving stretching surface with effects of variable thermal conductivity, Soret and Dufour numbers, as shown in Figure 1.

Two equal and opposite forces are applied along the x-axis so that the local tangential velocity is $u_w(x)=cx$, where c is a positive constant. The external stream is set into an impulsive motion from rest with the velocity $u_e(x)=ax$, where a > 0 is a constant. The temperature and the concentration of the ambient fluid are T_∞ and C_∞, and those at the stretching surface are T_w and C_w, respectively. With introducing Boussinesq approximations, the equations governing the steady-state conservation of mass, momentum,energy, and concentration for laminar boundary-layer flow can be written in two-dimensional Cartesian coordinates (x, y) as (Dulal [27], Hossain et al. [28] and Mukhopadhyay [29]):

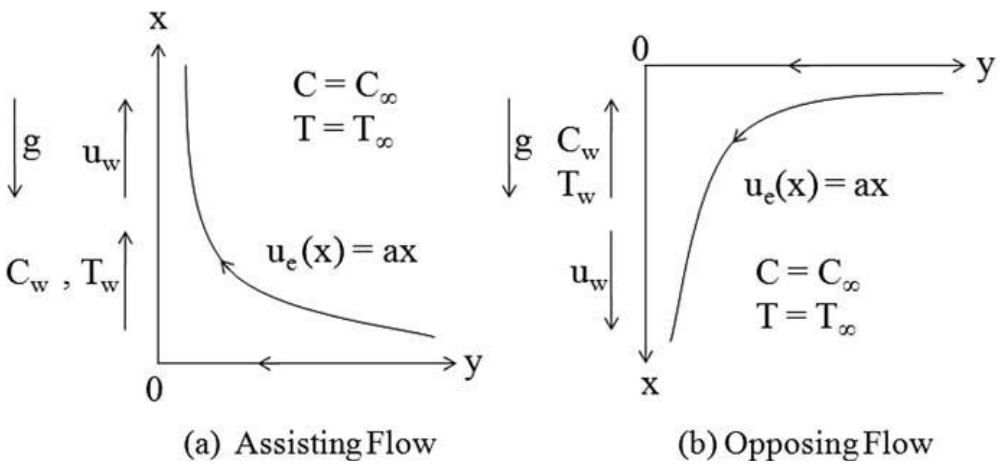

Figure 1: Geometry of the Problem and coordinates system

$$\frac{\partial u}{\partial x}+\frac{\partial v}{\partial y}=0 \qquad (1)$$

$$u\frac{\partial u}{\partial x} + v\frac{\partial u}{\partial y} = u_e\frac{du_e}{dx} + \nu\frac{\partial^2 u}{\partial y^2} \pm g\beta_T\,(T - T_\infty) \pm g\,\beta_C\,\,(C - C_\infty) \tag{2}$$

$$\rho c_p\left(u\frac{\partial T}{\partial x} + v\frac{\partial T}{\partial y}\right) = \frac{\partial}{\partial y}\left(k\frac{\partial T}{\partial y}\right) + \frac{D_m K_T}{C_s C_p}\frac{\partial^2 C}{\partial y^2} \tag{3}$$

$$u\frac{\partial C}{\partial x} + v\frac{\partial C}{\partial y} = D_m\frac{\partial^2 C}{\partial y^2} + \frac{D_m K_T}{T_m}\frac{\partial^2 T}{\partial y^2} \tag{4}$$

The boundary conditions for this problem can be written as

$$T=T_w(x)=T_\infty+bx,\quad u=u_w(x)=cx\quad,\ v=0, C=C_w(x)=C_\infty+dx,\quad \text{at } y=0 \tag{5}$$

$$u=u_e(x)=ax\ ,\ T\to T_\infty,\quad C\to C_\infty\ ,\quad \text{as}\quad y\to\infty$$

where u and v are the fluid velocity components along the x- and y- axes, T is the temperature of the fluid. C_p is the specific heat due to constant pressure. ρ is the density of the fluid. ν is the kinematics coefficients of viscosity. k is the fluid thermal diffusivity. g, β_T and β_c are the acceleration due to gravity, coefficient of thermal expansion and the coefficient of expansion with concentration respectively. a, b, c, d are constants and T_∞ is the temperature of the ambient fluid. D_m is the chemical molecular diffusivity. C is the concentration. The mass concentrations of the species at the wall C_w and that at infinity C_∞ are constants. u_w the stretching surface has linear velocity and u_e is the velocity of the flow external to the boundary layer. $K_T, C_s,$ T_m are the thermal diffusion ratio, concentration susceptibility and the mean fluid temperature. The "+" sign corresponds to an assisting flow while the "-"sign refers to an opposing flow.

Introducing the following similarity variables

$$\begin{aligned}&\psi=\sqrt{\nu c}\ xf(\eta)\ ,\ \eta=y\sqrt{\frac{c}{\nu}},\ T_w - T_\infty = bx,\\ &\theta=\frac{T-T_\infty}{T_w-T_\infty},\ C_w - C_\infty = dx\ ,\ \varphi=\frac{C-C_\infty}{C_w-C_\infty}\end{aligned} \tag{6}$$

where ψ is the stream function which is defined as following

$$u=\frac{\partial\psi}{\partial y},\ v=-\frac{\partial\psi}{\partial x} \tag{7}$$

Then from (6) into (7) we can get u and v as follows

$$u=c\,x\,f'(\eta),\ v=-(cv)^{\frac{1}{2}}\,f(\eta) \tag{8}$$

Following [28]-[29] the variation of thermal diffusivity is given as

$$k=k_{\infty}(1+\varepsilon\frac{T-T_{\infty}}{T_w-T_{\infty}}) \tag{9}$$

where ε is a parameter which depends on the nature of the fluid and k_{∞} is the value of thermal diffusivity at the temperature T_{∞}. By substituting from similarity variables Eq.(6), stream function Eq.(7), and thermal diffusivity Eq.(9) into equations (1)-(4) we get the following system of ordinary equations

$$f'''+f\,f''-f'^{2}\pm\lambda\theta\pm\delta\varphi+\frac{a^2}{c^2}=0 \tag{10}$$

$$(1+\varepsilon\theta)\theta''+\varepsilon\theta'^{2}+\Pr(f\theta'-f'\theta+D_f\varphi'')=0 \tag{11}$$

$$\varphi''+\mathrm{Le}(f\varphi'-f'\varphi+S_r\theta'')=0 \tag{12}$$

The boundary conditions (5) become

$$f(0)=0,\qquad f'(0)=1,\qquad \theta(0)=1,\qquad \varphi(0)=1 \tag{13}$$

$$f'(\infty)=\frac{a}{c},\qquad \theta(\infty)=0,\qquad \varphi(\infty)=0 \tag{14}$$

where λ is the thermal buoyancy parameter; Gr is the local Grashof number; Gc is the local solutal Grashof number; δ is the solutal buoyancy parameter; α is the coefficient of thermal diffusivity; Pr is the Prandtl number (ratio of viscous diffusion rate over thermal diffusion rate); Le is Lewis Number (the ratio of mass diffusivity to thermal diffusivity), Df is Dufour Number, Sr is Soret Number and Re_x is the local Reynolds number which are defined by

$$\lambda=\frac{Gr}{Re_x^2},\quad Gr=\frac{g\beta_T x^3(T_w-T_\infty)}{\nu^2},\quad S_r=\frac{D_m k_T(T_w-T_\infty)}{\nu T_m(C_w-C_\infty)},\quad Re_x=\frac{u_w x}{\nu},\quad Pr=\frac{\nu}{\alpha}$$

$$\delta=\frac{Gc}{Re_x^2},\quad Gc=\frac{g\beta_c x^3(C_w-C_\infty)}{\nu^2},\quad D_f=\frac{D_m k_T(C_w-C_\infty)}{C_s C_p \nu(T_w-T_\infty)},\quad \alpha=\frac{k}{\rho C_p},\quad Le=\frac{\alpha_m}{D_m}$$

The quantities of physical interest in this problem are the local skin friction coefficient, the local Nusselt number, and the local Sherwood numbers, which are defined by

$$C_f=\frac{\tau_w}{\rho u_w^2},\qquad Nu_x=\frac{xq_w}{k(T_w-T_\infty)},\qquad Sh_x=\frac{xq_m}{D_m(C_w-C_\infty)}, \tag{15}$$

where τ_w, q_w and q_m are the local wall shear stress, heat flux at the boundary, and mass flux at the boundary, which is given by

$$\tau_w=\mu\left(\frac{\partial u}{\partial y}\right)_{y=0},\qquad q_w=-\left(k\frac{\partial T}{\partial y}\right)_{y=0},\qquad q_m=-\left(D_m\frac{\partial C}{\partial y}\right)_{y=0}, \tag{16}$$

With μ being the dynamic viscosity, then from (6) and (16) into (15), we get

$$C_f\sqrt{Re_x}=f''(0),\qquad \frac{Nu_x}{\sqrt{Re_x}}=-\theta'(0),\qquad \frac{Sh_x}{\sqrt{Re_x}}=-\varphi'(0) \tag{17}$$

Definition 2.1 *This is a text of a definition.*

$$ax+by+c=0$$

3 Results and discussions

The set of non-linear ordinary differential equations (10)-(12) with boundary conditions (13)-(14) are integrated numerically by using Runge–Kutta method with a systematic guessing of $f''(0)=0$, $\theta'(0)=0$ and $\varphi'(0)=0$ by the Newton–Raphson shooting technique. The step size $\Delta\eta=0.001$ is used to obtain the numerical solution and the boundary condition $\eta\to\infty$ is approximated by

$\eta_{max} = 7$, and accuracy to the fifth decimal place is sufficient for convergence. In the numerical solution, a step size of $\Delta\eta = 0.001$ and $\eta_\infty = 7$ were found to be satisfactory for a convergence criterion of 10^{-5}. Numerical computations are carried out for $0 \le \lambda \le 3, 0 \le \delta \le 1, 0.2 \le S_r \le 0.75, 0.08 \le D_f \le 0.3, 0 \le a/c \le 5,$ $0 \le \varepsilon \le 0.5, 0.72 \le Pr \le 3$ and $0.5 \le Le \le 4$. In order to assess the accuracy of the numerical method, we have compared our local skin friction coefficient represented by $f''(0)$ with the previously published data Mahapatra and Gupta [13], Nazar et al. [30], Ishak et al. [15] and Pal [27] for selected values of a/c with $\lambda=\delta=\varepsilon=D_f=S_r=Le=0$. The comparison is listed in table 1, and it is found to be in excellent agreement. This degree of closeness vouches for the high accuracy of the present computational scheme. Finally, the values of local skin friction coefficient $f''(0)$ and local Nusselt number $\theta'(0)$ are compared with Ishak et al. [15] and Pal [27] for several values of Pr when $a/c=\lambda=1$ with $\delta=\varepsilon=D_f=S_r=Le=0$ for assisting and opposing flows are shown in table 2 and table 3, respectively. In each case we found an excellent agreement. In closing the discussion, the wall shear stress, local rate of heat transfer and local mass transfer rate are, respectively, measured in terms of the local skin friction coefficients, the local Nusselt number and local the Sherwood number. Finally the numerical results for different values of the controlling parameters are tabulated in Table 4. From Table 4, it is clear that the shear stress, the rate of heat and mass transfer increase by increasing of λ and δ in the case of assisting flow whereas reverse trend is seen for opposing flow. Due to the increase value of a/c, it is found that the shear stress, the rate of heat and mass transfer increase in both cases of assisting and opposing flows. The shear stress and the rate mass transfer decrease whereas the rate of heat transfer increases by increasing Pr in the case of assisting flow. Moreover, it is observed that the shear stress and the rate heat transfer increase whereas the rate of mass transfer decreases by increasing Pr in the case of opposing flow. The shear stress and the rate mass transfer increase whereas the

rate of heat transfer decreases by increasing ε in the case of assisting flow. Moreover, it is observed that the shear stress and the rate heat transfer decrease whereas the rate of mass transfer increases by increasing ε in the case of opposing flow. The shear stress and the rate heat transfer decrease whereas the rate of mass transfer increases by increasing Le in the case of assisting flow. Moreover, it is observed that the shear stress and the rate heat transfer increase whereas the rate of mass transfer decreases by increasing Le in the case of opposing flow. Finally, it is observed that the local rate of heat transfer increases whereas the shear stress and the local mass transfer rate decrease when the Soret number Sr increases and the Dufour number Df decreases simultaneously, in both cases of assisting and opposing flows. Figures 2-22, are drawn in order to see the influence of thermal buoyancy parameter λ, the solutal buoyancy parameter δ, the thermal diffusivity parameter ε, the ratio a/c, Prandtl number Pr, Lewis Number Le, Dufour Number Df, and Soret Number Sr on the velocity, temperature and concentration distributions for both cases of assisting and opposing flows. Figures 2-4 show that the effect of thermal buoyancy parameter on the velocity, temperature, and concentration respectively. As shown for assisting flow the temperature and the concentration are slightly decreasing with increasing λ, whereas the velocity increases as λ increases. For opposing flow the effect of λ is larger than in assisting flow case, and takes the reverse trend with all. Figures 5-7 show that the effect of solutal buoyancy parameter on the velocity, temperature, and concentration respectively. It's clear for assisting flow the temperature and the concentration are slightly decreasing with increasing δ, whereas the velocity increases as δ increases. Moreover, the reverse trend is seen for opposing flow. Figures 8-10 illustrate the effect of the ratio a/c on the velocity, temperature, and concentration distributions. For both assisting and opposing flows the temperature and the concentration distributions are decreasing with increasing a/c. In the other hand, the velocity increases as a/c increases. If $a/c < 1$ there is a significant effect depends on the type of the flow (assisting or

opposing) as shown in the velocity distributions Figure 8, whereas if $a/c >> 1$ this effect may be vanished. Physically that means if the velocity of the flow far from the boundary layer u_e is less than the stretching sheet velocity u_w, then the effect of the type of the flow (assisting or opposing) appears clearly for the velocity, temperature, and concentration, whereas if $u_e >> u_w$ may be there is slightly or no difference in the behaviors of these fluid properties for both. The influence of the thermal diffusivity parameter ε on the velocity, temperature, and concentration is displayed in Figures 11-13. It's clear that for assisting flow the velocity distributions increases as ε increases, whereas the reverse trend is seen for opposing flow. Also, the temperature distributions increase as ε increases in both cases of assisting and opposing flows. Moreover, the concentration distributions are not sensitive with increase of ε. Figures 14-16, show the velocity, temperature, and concentration distributions for various values of Prandth number for both cases assisting and opposing flows, respectively. It's clear that for opposing flow the velocity distributions increase as Pr increases whereas the reverse trend is seen for assisting flow. Also, the temperature and concentration distributions decrease as Pr increases for both cases of assisting and opposing flows. Figures 17-19, show the velocity, temperature, and concentration distributions for various values of Lewis Number for both cases assisting and opposing flows, respectively. It's clear that for opposing flow the velocity distributions increase as Le increases whereas the reverse trend is seen for assisting flow. It is observed that the temperature distributions at any point near the plate slightly increases by increasing Le whereas the opposite is observed further away from the plate for assisting and opposing flows. Moreover, the concentration distributions decrease as Le increases in both cases of assisting and opposing flows. Figures 20-22, show the velocity, temperature and the concentration distributions for various values of the Soret number Sr increases and the Dufour number Df decreases simultaneously. It's clear that for assisting flow the velocity distributions increase with the variation of Df and Sr whereas the

reverse trend is seen for opposing flow. Finally, the concentration distributions increase with the variation of Df and Sr whereas the reverse trend is seen for temperature distributions in both cases of assisting and opposing flows.

4 Labels of figures and tables

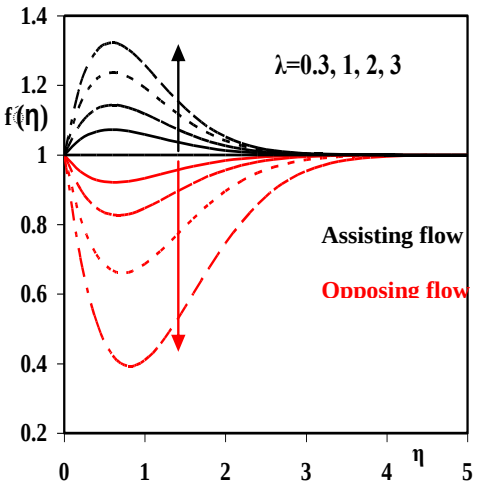

Figure 2: Effect of λ on the velocity for δ=0.5, a/c=1, Pr=0.72, Le=1, ε=0.4, Sr=0.2 and Df=0.3

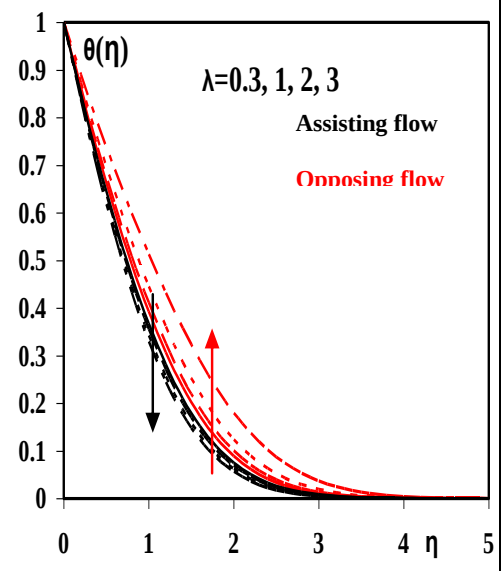

Figure 3: Effect of λ on the temperature θ(η) for δ=0.5, a/c=1, Pr=0.72, Le=1, ε=0.4, Sr=0.2 and Df=0.3

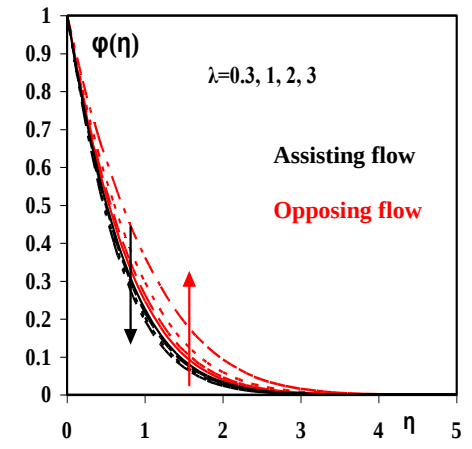

Figure 4: Effect of λ on the concentration φ(η) for δ=0.5, a/c=1, Pr=0.72, Le=1, ε=0.4, Sr=0.2 and Df=0.3

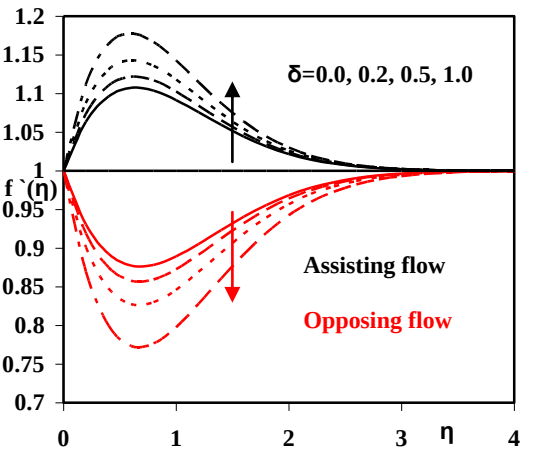

Figure 5: Effect of δ on the velocity for λ =1., a/c=1, Pr=0.72, Le=1, ε=0.4, Sr=0.2 and Df=0.3

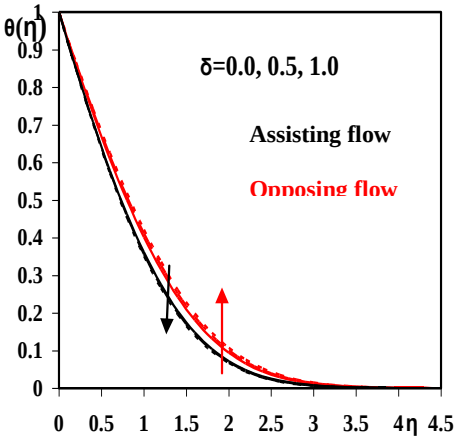

Figure 6: Effect of δ on the temperature θ(η) for λ =1, a/c=1, Pr=0.72, Le=1, ε=0.4, Sr=0.2 and Df=0.3

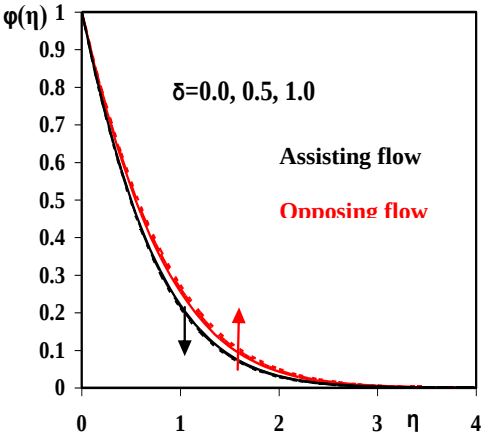

Figure 7: Effect of δ on the concentration φ(η) for λ =1, a/c=1, Pr=0.72, Le=1, ε=0.4, Sr=0.2 and Df=0.3

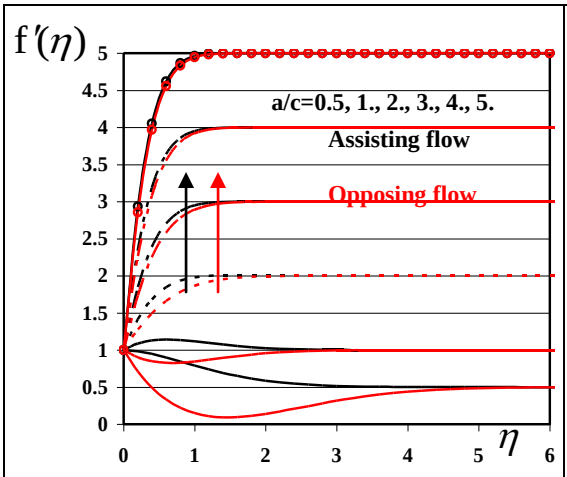

Figure 8: Effect of a/c on the velocity for δ=0.5, λ =1, Pr=0.72, Le=1, ε=0.4, Sr=0.2 and Df=0.3

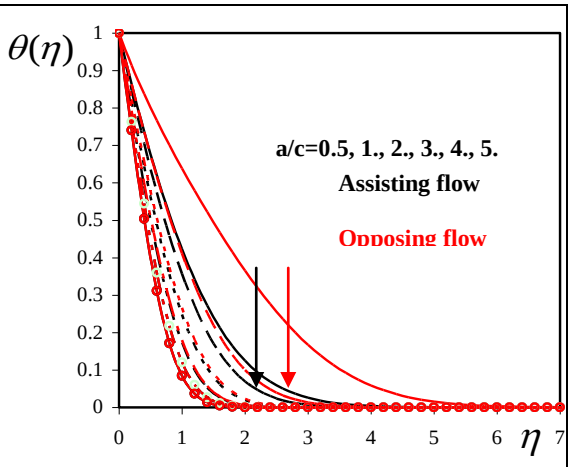

Figure 9: Effect of a/c on the temperature θ(η) for δ =0.5, λ =0.5, Pr=0.72, Le=1, ε=0.4, Sr=0.2 and Df=0.3

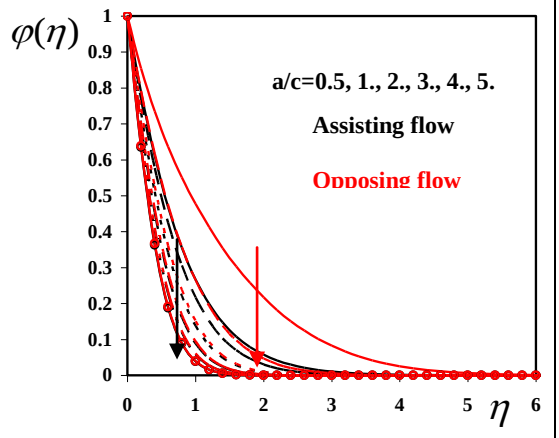

Figure 10: Effect of a/c on the concentration φ(η) for δ=.5, λ =1, Pr=0.72, Le=1, ε=0.4, Sr=0.2 and Df=0.3

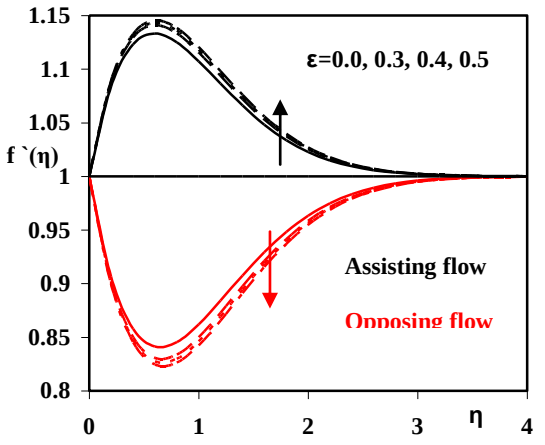

Figure 11: Effect of ε on the velocity for δ=0.5, λ =1, Pr=0.72, Le=1, a/c =1., Sr=0.2 and Df=0.3

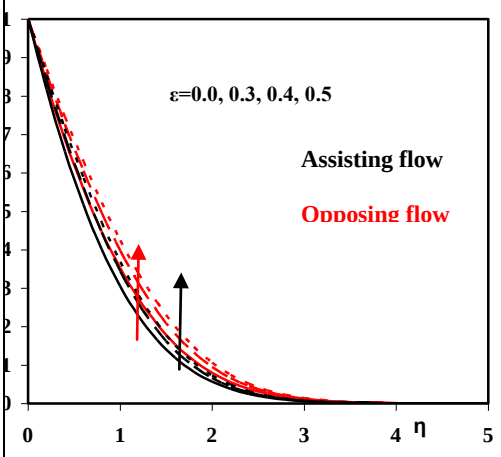

Figure 12: Effect of ε on the temperature θ(η) for δ =0.5, λ =0.5, Pr=0.72, Le=1, a/c =1, Sr=0.2 and Df=0.3

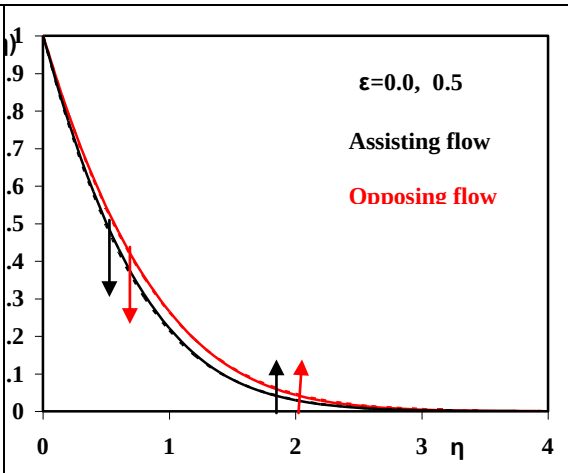

Figure13: Effect of ε on the concentration φ(η) for δ =0.5, λ =0.5, Pr=0.72, Le=1, a/c =1, Sr=0.2 and Df=0.3

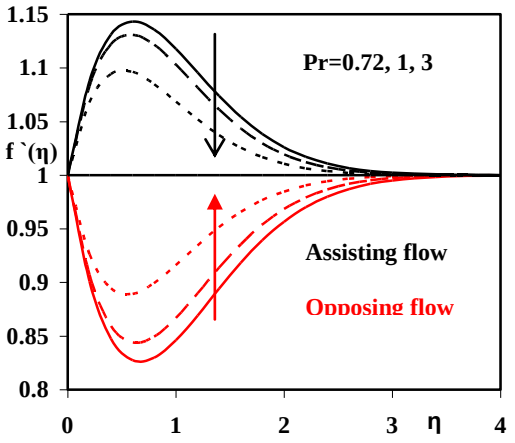

Figure 14: Effect of Pr on the velocity for δ =0.5, λ =1, Sr=0.2, Le=1, a/c =1., Df=0.3 and ε =0.4

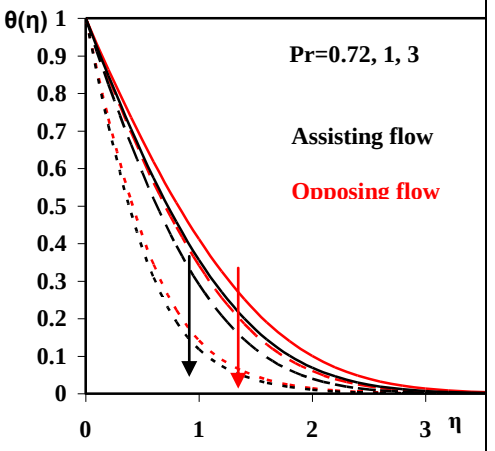

Figure 15: Effect of Pr on the temperature θ(η) for δ =0.5, oλ =1, Sr=0.2, Le=1, a/c =1., Df=0.3 and ε =0.4

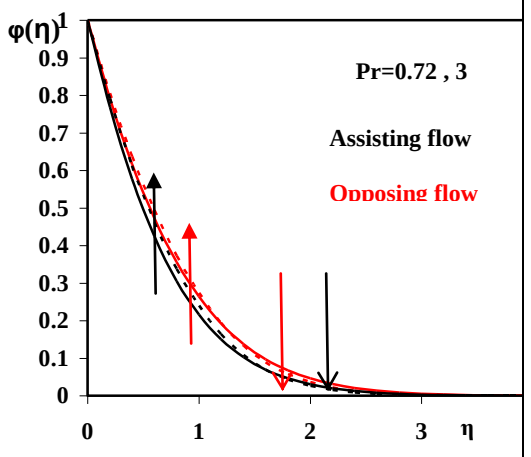

Figure 16: Effect of Pr on the concentration φ(η) for δ=0.5, λ =1, Sr=0.2, Le=1, a/c =1., Df=0.3 and ε =0.4

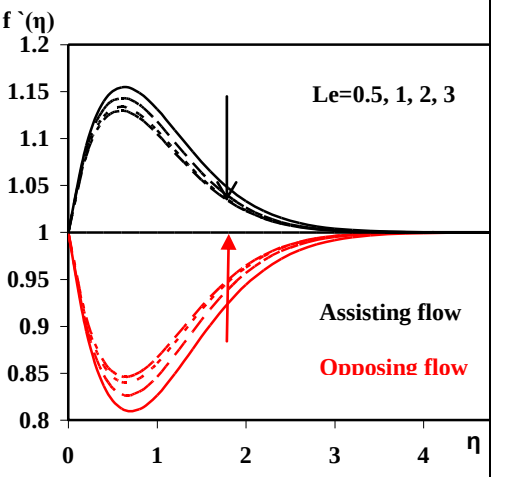

Figure 17: Effect of Le on the velocity for δ =0.5, λ =1, Sr=0.2, Pr=0.72, a/c =1., Df=0.3 and ε =0.4

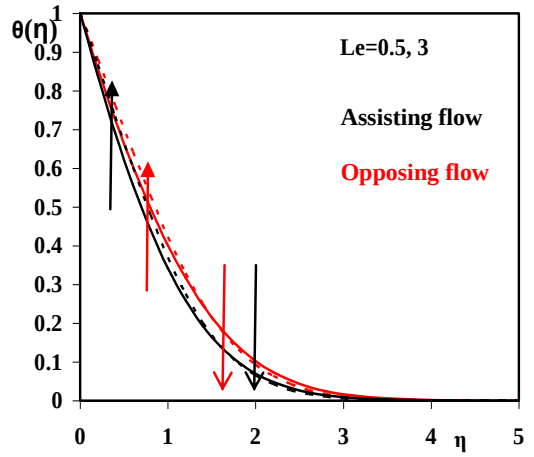

Figure 18: Effect of Le on the temperature θ(η) for δ =0.5, λ =1, Sr=0.2, Pr=0.72, a/c =1., Df=0.3 and ε =0.4

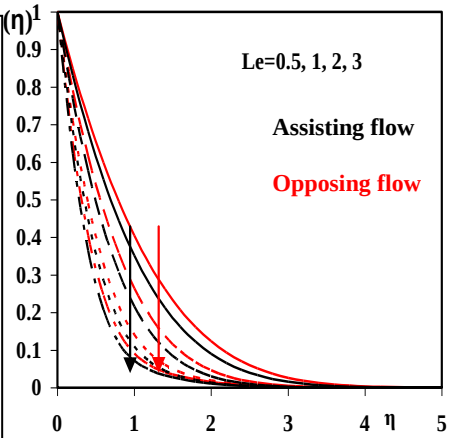

Figure 19: Effect of Pr on the concentration φ(η) for δ=0.5, λ =1, Sr=0.2, Pr=0.72, a/c =1., Df=0.3 and ε =0.4

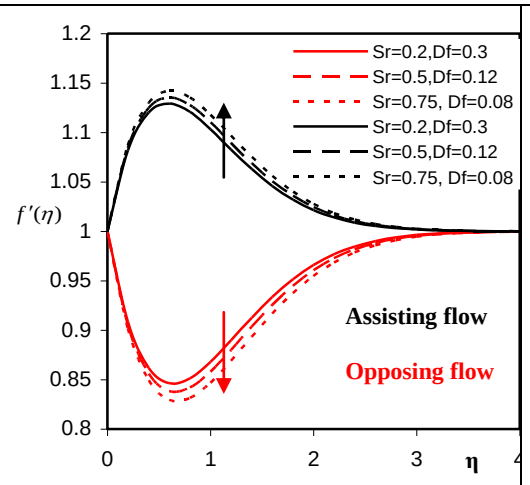

Figure 20: Effect of Sr and Df on the velocity for δ =0.5, λ =1, Pr=0.72, Le=1, a/c =1., and ε =0.4

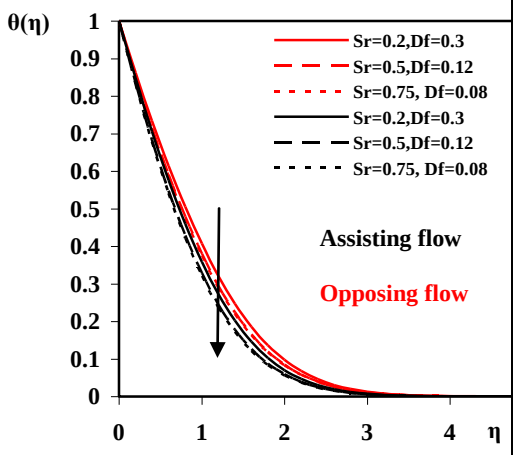

Figure 21: Effect of Sr and Df on the temperature θ(η) for δ =0.5, λ =1, Pr=0.72, Le=1, a/c =1., and ε =0.4

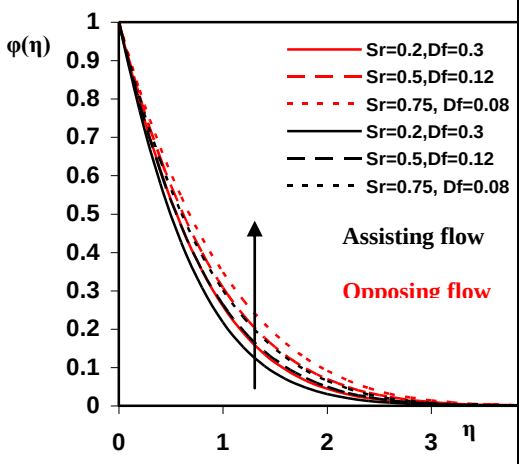

Figure 22: Effect of Sr and Df on the concentration φ(η) for δ=0.5, λ =1, Pr=0.72, Le=1, a/c =1., and ε =0.4

Table 1: Values of $C_f R_{e_x}^{1/2}$ for different values of a/c in absence of buoyancy forces λθ and δφ

a/c	Mahapatra and Gupta[13]	Nazar et al. [30]	Ishak et al. [15]	Dulal Pal [27]	Present results
0.1	-0.9694	-0.9694	-0.9694	-0.96939	-0.9694
0.2	-0.9181	-0.9181	-0.9181	-0.91811	-0.9181
0.5	-0.6673	-0.6673	-0.6673	-0.66726	-0.6673
2.0	2.0175	2.0176	2.0175	2.01750	2.0175
3.0	4.7293	4.7296	4.7294	4.72928	4.7292

Table 2: Values of $C_f R_{e_x}^{1/2}$ and $Nu_x / R_{e_x}^{1/2}$ for different values of Pr in absence of buoyancy forces δφ when a/c=1 and λ=1 for assisting flow

	Ishak et al. [15]		Dulal Pal [27]		Present results	
Pr	$C_f R_{e_x}^{1/2}$	$Nu_x / R_{e_x}^{1/2}$	$C_f R_{e_x}^{1/2}$	$Nu_x / R_{e_x}^{1/2}$	$C_f R_{e_x}^{1/2}$	$Nu_x / R_{e_x}^{1/2}$
0.72	0.3645	1.0931	0.36449	1.09311	0.3645	1.0931
6.8	0.1804	3.2902	0.18042	3.28957	0.1804	3.2894
20.	0.1175	5.6230	0.11750	5.62014	0.1173	5.6182
40.	0.0873	7.9463	0.08724	7.93831	0.0845	7.9383
60	0.0729	9.7327	0.07284	9.71801	0.0682	9.7141
80.	0.0640	11.2413	0.06394	11.21875	0.0572	11.2205
100.	0.0578	12.5726	0.05773	12.54113	0.0491	12.5829

Table 3: Values of $C_f R_{e_X}^{1/2}$ and $Nu_x / R_{e_X}^{1/2}$ for different values of Pr in absence of buoyancy forces δφ when a/c=1 and λ=1 for opposing flow

	Ishak et al. [15]		**Dulal Pal [27]**		**Present results**	
Pr	$C_f R_{e_X}^{1/2}$	$Nu_x / R_{e_X}^{1/2}$	$C_f R_{e_X}^{1/2}$	$Nu_x / R_{e_X}^{1/2}$	$C_f R_{e_X}^{1/2}$	$Nu_x / R_{e_X}^{1/2}$
0.72	-0.3852	1.0293	-0.38519	1.02925	-0.3852	1.0293
6.8	-0.1832	3.2466	-0.18323	3.24609	-0.1832	3.246
20.	-0.1183	5.5923	-0.11831	5.58960	-0.1182	5.5878
40.	-0.0876	7.9277	-0.08758	7.91491	-0.0856	7.9077
60	-0.0731	9.7126	-0.07304	9.69818	-0.0685	9.6961
80.	-0.0642	11.2235	-0.06408	11.20118	-0.0545	11.3026
100.	-0.0579	12.5564	-0.05783	12.52519	-0.046	12.7356

Table 4: Values of $C_f R_{e_x}^{1/2}$, $Nu_x / R_{e_x}^{1/2}$ and $\frac{\mathrm{Sh}_x}{\mathrm{Ra}_x^{1/2}}$

								Assisting flow			Opposing flow		
Λ	δ	a/c	Pr	ε	Le	Df	Sr	$f''(0)$	$-\theta'(0)$	$-\varphi'(0)$	$f''(0)$	$-\theta'(0)$	$-\varphi'(0)$
1.0	0.5	1.0	0.72	0.4	1.0	0.3	0.2	0.5761	0.7844	1.2552	-0.6332	0.7036	1.1349
						0.12	.5	0.5735	0.8532	1.1522	-0.6297	0.7675	1.0411
						0.08	0.75	0.5785	0.8691	1.0675	-0.6362	0.7806	0.9613
					0.5	0.3	0.2	0.5997	0.8306	0.8926	-0.6638	0.7395	0.7955
					1.0			0.5761	0.7844	1.2552	-0.6332	0.7036	1.1349
					2.0			0.5539	0.7133	1.7785	-0.6048	0.6413	1.6355
					4.0			0.5337	0.6010	2.5650	-0.5796	0.5362	2.4013
				0.0	1.0			0.5534	0.9700	1.2237	-0.6041	0.879	1.1139
				0.3				0.5710	0.8209	1.2492	-0.6265	0.7381	1.1312
				0.4				0.5761	0.7844	1.2552	-0.6332	0.7036	1.1349
				0.5				0.5810	0.7524	1.2605	-0.6395	0.6733	1.1379
			0.72	0.4				0.5761	0.7844	1.2552	-0.6332	0.7036	1.1349
			1.0					0.5511	0.9116	1.2350	-0.6012	0.8272	1.1259
			3.0					0.4714	1.5373	1.1289	-0.5030	1.4444	1.0508

Table 4 : (continued) Values of $C_f R_{e_x}^{1/2}$, $Nu_x / R_{e_x}^{1/2}$ and $\frac{\mathrm{Sh}_x}{\mathrm{Ra}_x^{1/2}}$

								Assisting flow			Opposing flow		
Λ	δ	a/c	Pr	ε	Le	Df	Sr	$f''(0)$	$-\theta'(0)$	$-\varphi'(0)$	$f''(0)$	$-\theta'(0)$	$-\varphi'(0)$
1.0	0.5	1.0	3.0	0.4	1.0	0.3	0.2	0.4714	1.5373	1.1289	-0.5030	1.4444	1.0508
		0.5	0.72					-0.0093	0.7062	1.1579	-1.6612	0.4575	0.8143
		1.0						0.5761	0.7844	1.2552	-0.6332	0.7036	1.1349
		2.0						2.4868	0.9378	1.4596	1.5328	0.9014	1.4034
		3.0						5.1336	1.0754	1.6499	4.3182	1.0535	1.6155
	0.0	1.0						0.4102	0.7757	1.2419	-0.439	0.7171	1.1553
	0.5							0.5761	0.7844	1.2552	-0.6332	0.7036	1.1349
	1.0							0.7391	0.7928	1.2679	-0.8355	0.6886	1.1123
0.3	0.5							0.2976	0.7671	1.2297	-0.3113	0.7286	1.1718
1.0								0.5761	0.7844	1.2552	-0.6332	0.7036	1.1349
2.0								0.9585	0.8066	1.2880	-1.1430	0.6574	1.0668
3.0								1.3261	0.8264	1.3174	-1.8028	0.5749	0.9449

5 Conclusion

The present work helps us understanding numerically as well as physically the stagnation-point phenomenon on free heat and mass transfer flow of an incompressible fluid over stretching sheet in the presence of variable thermal conductivity with Soret and Dufour effects. The governing equations are reduced to a system of nonlinear ordinary differential equations by using suitable similarity transformations. These equations are more conveniently solved numerically by using fourth order Runge-Kutta integration scheme with Newton Raphson shooting method for a wide range of parameters. A comparison with previously published work is performed and the results are found to be in good agreement. Based on the obtained results, the following conclusions may be drawn:

1- The shear stress, the rate of heat and mass transfer increase by increasing of λ and δ in the case of assisting flow whereas reverse trend is seen for opposing flow.

2- The shear stress, the rate of heat and mass transfer increase by increasing of a/c in both cases of assisting and opposing flows.

3- The shear stress and the rate mass transfer increase whereas the rate of heat transfer decreases by increasing ε in the case of assisting flow. Moreover, it is observed that the shear stress and the rate heat transfer decrease whereas the rate of mass transfer increases by increasing ε in the case of opposing flow.

4- The local rate of heat transfer increases whereas the shear stress and the local mass transfer rate decrease when the Soret number Sr increases and the Dufour number Df decreases simultaneously in both cases of assisting and opposing flows.

ACKNOWLEDGEMENTS. This work was supported by the Deanship of Scientific Research in Salman Bin Abdulaziz University, Saudi Arabia under Grants No.1432/هـ/ 18.

References

[1] B.C. Sakiadis, Boundary layer behavior on continuous solid surface, *AIChE J*., **7**, (1961), 26-28.

[2] L.J. Crane, Flow past a stretching plate, *Z. Angew. Math. Phys*., **21**, (1970), 645-647.

[3] L.J. Grubka and K.M. Bobba, Heat transfer characteristics of a continuous stretching surface with variable temperature, *Trans. ASME, J. Heat Transfer*, **107**, (1985), 248-250.

[4] R. Cortell, Flow and heat transfer of a fluid through a porous medium over a stretching surface with internal heat generation/absorption and suction/blowing, *Fluid Dynam. Res*., **37**, (2005), 231-245.

[5] R. Cortell, Internal heat generation and radiation effects on a certain free convection flow, *Int. J. Nonlinear Sci*., **9**, (2010), 468-479.

[6] R. Cortell, Effects of viscous dissipation and radiation on the thermal boundary layer over a nonlinearly stretching sheet, *Phys. Lett. A*, **372**, (2008), 631-636.

[7] A. Ishak, R. Nazar and I. Pop, Heat transfer over an unsteady stretching permeable surface with prescribed wall temperature, *Nonlinear Anal. Real World Appl*., **10**, (2009), 2909-2913.

[8] Z. Ziabakhsh, G. Domairry, M. Mozaffari and M. Mahbobifar, Analytical solution of heat transfer over an unsteady stretching permeable surface with prescribed wall temperature, *J. Taiwan Inst. Chem. Eng*., **41**, (2010), 169-177.

[9] T. Fang, Flow and heat transfer characteristics of the boundary layers over a stretching surface with a uniform-shear free stream, *Int. J. Heat Mass Transfer*, **51**, (2008), 2199- 2213.

[10] R. Cortell, Heat and fluid flow due to non-linearly stretching surfaces, *Applied Mathematics and Computation*, **217**, (2011), 7564-7572.

[11] K. Hiemenz, Die Grenzschicht an einem in den gleichformigen

Fluessigkeitsstrom eingetauchten geraden Kreiszylinder, *Dinglers Polytechnisches J.*, **326**, (1911), 321-410.

[12] T. Chiam, Stagnation-point flow towards a stretching plate, *J. Phys. Soc. Jpn.*, **63**(6), (1994), 2443-2444.

[13] T.R. Mahapatra and A.S. Gupta, Heat transfer in stagnation-point flow towards a stretching sheet, *Heat Mass Transfer*, **38**, (2002), 517-521.

[14] A. Ishak, R. Nazar and I. Pop, Mixed convection boundary layers in the stagnationpoint flow toward a stretching vertical sheet, *Meccanica*, **41**, (2006), 509-518.

[15] A. Ishak, R. Nazar and I. Pop, Dual solutions in mixed convection flow near a stagnation point on a vertical surface in a porous medium, *Int. J. Heat Mass Tran.*, **51**(5-6), (2008), 1150-1155.

[16] G.C. Layek, S. Mukhopadhyay and Sk. A. Samad, Heat and mass transfer analysis for boundary layer stagnation-point flow towards a heated porous stretching sheet with heat absorption/generation and suction/blowing, *Int. Commun. Heat Mass Transfer*, **34**, (2007), 347-356.

[17] S. Nadeem, A. Hussain and M. Khan, HAM solutions for boundary layer flow in the region of the stagnation point towards a stretching sheet, *Commun. Nonlinear Sci. Numer. Simul.*, **15**, (2010), 475-481.

[18] M.M. Rashidi and E. Erfani, A new analytical study of MHD stagnation–point flow in porous media with heat transfer, *Computers & Fluids*, **40**, (2011), 172-178.

[19] A.A. Afify and N.S. Elgazery, Lie group analysis for the effects of chemical reaction on MHD stagnation-point flow of heat and mass transfer towards a heated porous stretching sheet with suction or injection, *Nonlinear Anal. Model. Control*, **17**, (2012), 1-15.

[20] J.A. Weaver and R. Viskanta, Natural Convection due to Horizontal Temperature and Concentration Gradients. Species Interdiffusion, Soret and Dufour Effects, *Int. J. Heat Mass Transfer*, **34**, (1991), 3121-3133.

[21] Z. Dursunkaya and W.M. Worek, Diffusion-thermo and thermal-diffusion effects in transient and steady natural convection from vertical surface, *Int. J. Heat MassTransfer*, **35**, (1992), 2060-2067.

[22] A.J. Chamkha and A. Ben-Nakhi, MHD Mixed convection-radiation interaction along a permeable surface immersed in a porous medium in the presence of Soret and Dufour's Effect, *Heat Mass Transfer*, **44**, (2008), 845-856.

[23] M.A. Seddeek, Thermal-diffusion and diffusion-thermo effects on mixed free forced convective flow and mass transfer over accelerating surface with a heat source in the presence of suction and blowing in the case of variable viscosity, *Acta Mech*., **172**, (2004), 83-94.

[24] A.A. Afify, Similarity solution in MHD: Effects of thermal diffusion and diffusion thermo on free convective heat and mass transfer over a stretching surface considering suction or injection, *Commun Nonlinear Sci Numer Simulat*, **14**, (2009), 2202-2214.

[25] Adrian Postelnicu, Heat and mass transfer by natural convection at stagnation point in a porous medium considering Soret and Dufour effects, *Heat Mass Transfer*, **46**, (2010), 831-840.

[26] E. Magyari and A. Postelnicu, Double diffusive natural convection flows with thermosolutal symmetry in porous media in the presence of the Soret-Dufour effects, *Transport in Porous Media*, **88**, (2011), 149-167.

[27] Dulal Pal, Heat and mass transfer in stagnation-point flow towards a stretching surface in the presence of buoyancy force and thermal radiation, *Meccanica*, **44**, (2009), 145-158.

[28] Md.A. Hossain, Md.S. Munir and D.A.S. Rees,Flow of viscous incompressible fluid with temperature dependent viscosity and thermal conductivity past a permeable wedge with uniform surface heat flux, *Int. J. Therm. Sci*., **39**, (2000), 635-644.

[29] S. Mukhopadhyay, Unsteady boundary layer flow and heat transfer past a

porous stretching sheet in presence of variable viscosity and thermal diffusivity, *Heat Mass Transfer*, **52**, (2009), 5213-5217.

[30] R. Nazar, N. Amin, D. Flip and I. Pop, Unsteady boundary layer flow in the region of the stagnation point on a stretching sheet, *Int. J. Eng Sci*., **42**, (2004), 1241-1253.